Korean J. Chem. Eng., **21**(3), 733-738 (2004)

Growth Mechanism of Needle-shaped ZnO Nanostructures over NiO-coated Si Substrates

Tae Yun Kim, Seung Hyun Lee, Young Hwan Mo, Kee Suk Nahm†, Ji Young Kim*, Eun Kyung Suh* and Moon Kim**

Nano Materials Research Center and School of Chemical Engineering and Technology,
Chonbuk National University, Chonju 561-756, Republic of Korea
*Department of Semiconductor Science Technology, Chonbuk National University, Chonju 561-756, Republic of Korea
**Department of Materials Science, University of North Texas, P.O. Box 305310, Denton, Texas 76203-5310, USA
(*Received 2 September 2003 • accepted 20 November 2003*)

Abstract–ZnO nanostructures were synthesized over NiO-coated Si substrate by a thermal evaporation of Zn powders in a vertical chemical vapor deposition reactor. The ZnO nanostructures had a needle-like morphology and the diameter of the structures decreased linearly from the bottom to the top. The bottom diameters of the ZnO nano-needles normally ranged from 20-100 nm and the lengths were in the range of 2-3 μm. The clear lattice fringes in HRTEM image indicated the growth of good quality hexagonal single-crystal ZnO. Field emission characteristics of the ZnO nano-needles showed that the turn-on field was about 8.87 V/μm with a field enhancement factor of about 1099. The growth mechanism of the ZnO nano-needles was proposed on the basis of experimental data.

Key words: ZnO Nanostructures, Nano-needles, Evaporation of Zn, Characterization, Growth Mechanism

INTRODUCTION

Nanoscale one-dimensional materials such as nanotubes and nanowires have been successfully synthesized and have received much attention due to their extraordinary physical properties and potential application for nanodevices [Yang et al., 2002; Nahm et al., 2003; Park et al., 2002]. Owing to exceptional physical properties of ZnO such as high conductance, chemical and thermal stability, wide band-gap, and high piezoelectric coupling coefficient, it has been studied for piezoelectric devices and short wavelength (green/green blue) electro-optical devices [Zheng et al., 2002; Wang et al., 2002]. Electron field emitters in field-emission flat panel displays (FED) are another potential application area of semiconductor nanowires or nanotubes [Zhu et al., 1999; Lee et al., 2002]. Some wide band-gap semiconductors were reported as good electron field emitters because they have a high mechanical strength, and chemical stability [Frederick et al., 1999; Chen et al., 2001; Wu et al., 2002; Liu et al., 2002; Sohn et al., 2000; Kim et al., 2001]. The synthesis of one-dimensional ZnO material has been carried out using various methods such as arc-discharge [Choi et al., 2000], laser vaporization [Wu et al., 2002], template-based methods [Zhu and Fan, 1999; Li et al., 2000], high temperature physical evaporation [Wang et al., 2002] and reduction and oxidation of ZnS [Hu et al., 2002]. Most of the previous works have reported the growth of ZnO nanowires and nanobelts. Recently, relatively few papers [Park et al., 2002; Lee et al., 2003; Zhu et al., 2003; Tseng et al., 2003] have reported the growth of needle-like ZnO nanostructures, and the growth mechanism of the ZnO nano-needles has not been fully understood in the works.

In this work, we report the synthesis of needle-shaped ZnO nanostructures over NiO-coated Si substrate in a vertical chemical vapor deposition (CVD) reactor. The ZnO nanostructures were grown by thermal evaporation process of Zn powders under N_2 flow. The structural and electrical properties of the grown needle-like ZnO nanostructures were investigated by using various analytic techniques. The growth mechanism of the ZnO nano-needles was proposed on the basis of experimental results.

EXPERIMENTAL

ZnO nanostructures were synthesized by using a vertical CVD reactor depicted in Fig. 1 [Ahn et al., 2002]. The surface of Si (100) substrate (1.5 cm×6 cm) was first scratched with a fine sand paper to hold NiO well on the substrate and was then sonicated in acetone. A solution of 0.01 M $Ni(NO_3)_2 \cdot 6H_2O$ dissolved in ethanol was dropped on the cleaned Si surface. Then $Ni(NO_3)_2$-coated Si substrate was dried in an oven for 24 hr. Metal Zn powders (2 g) were loaded in an inner reactor and then the $Ni(NO_3)_2$-coated Si substrate was vertically set up over the Zn source. The inner reactor was placed

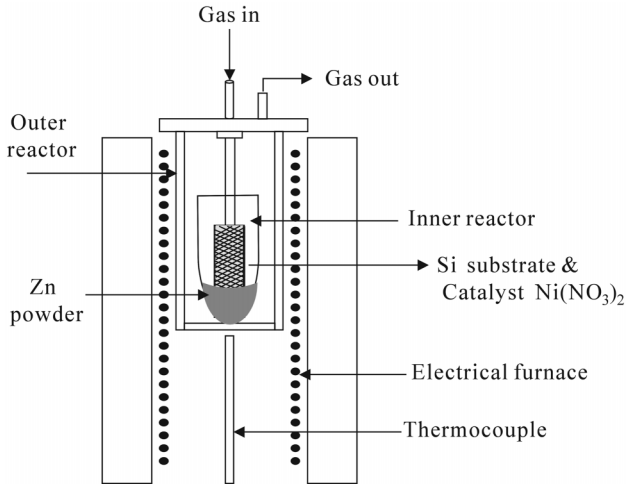

Fig. 1. A schematic diagram of the vertical chemical vapor deposition system for the growth of ZnO nano-needles.

†To whom correspondence should be addressed.
E-mail: nahamks@moak.chonbuk.ac.kr

in an outer quartz reactor. Nitrogen gas was introduced into the outer reactor through a delivery tube and the temperature of the furnace was heated to 500 °C under 20 sccm N_2 (99.99%) gas flow. It was reported that $Ni(NO_3)_2$ readily decomposes at ~260 °C to be NiO [Llewellyn et al., 1997]. The growth of ZnO nanostructures was carried out at 500 °C under N_2 gas flow. After the growth reaction, light ash-colored materials were found on the surface of the substrate and the materials were uniformly deposited at 2-4 cm distance between Zn source and substrate. The flow of N_2 gas was maintained during the reaction and the reactor was cooled to room temperature under the N_2 flow.

RESULTS AND DISCUSSION

ZnO nanostructures were grown for 60 min at 500 °C under N_2 gas flow at different reaction times. Light ash-colored materials were deposited on Si surface and were characterized by using XRD measurements. Fig. 2 shows an XRD pattern of the deposited materials on NiO coated Si substrate. The spectrum is almost equal to the typical XRD spectrum of ZnO reported in the previous papers [Lee et al., 2003; Sun et al., 2002]. The spectrum shows peaks at 2θ= 31.2, 33.88, 35.64, 47, 56.04, and 62.48 for ZnO (1010), ZnO (0002), ZnO (1011), ZnO (1012), ZnO (1120), and ZnO (1013), respectively. The diffraction peaks are indexed to be a wurtzite structure of ZnO and the strong intensities of the peaks present the growth of ZnO crystalline. It is not found that there are any other peaks due to the presence of unreacted Zn and other impurities except for Si substrate peak at 2θ=33.1, 61.2, 69.132 for Si (002), Si (004) K_β, and Si (004), respectively [Kim et al., 2001; Boo et al., 2000]. All the samples prepared in this experiment showed the similar XRD patterns, indicating the growth of ZnO crystalline. The ZnO nanostructure lattice constants calculated from the XRD data by using the Rietveld refinement method were a=3.241 and c=5.190 Å, consistent with those of bulk ZnO (JCPDS 75-0576).

Shown in Fig. 3 is an FE-SEM image for ZnO nanostructures grown on silicon substrate. The image presents the growth of vertically aligned ZnO nanostructures with high regularity and density. It is interesting to note that the diameter of the nanostructures decreases with increasing the length of the nanostructures from the bottom to the top to form a needle-shaped structure. The tip of the ZnO nano-needles is well developed without the formation of metal or metal oxide tips. EDX analysis also identified the absence of Ni or NiO on the sharpened tips. This result proposes that the nano-needles grow upward from the substrate surface. The diameter of the nano-needles normally ranges from 20-100 nm and the lengths are 3-5 μm long, though the diameter decreases as they grow.

Fig. 4(a) is a TEM image for the grown ZnO nano-needles. The

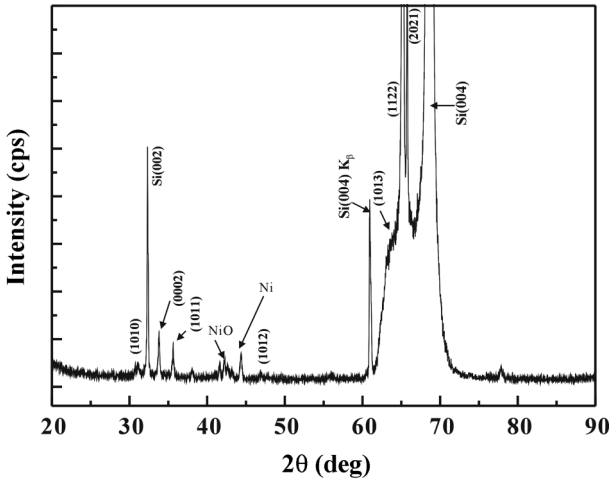

Fig. 2. A typical X-ray diffraction pattern of ZnO nano-needles grown at 500 °C for 60 min under N_2 gas flow.

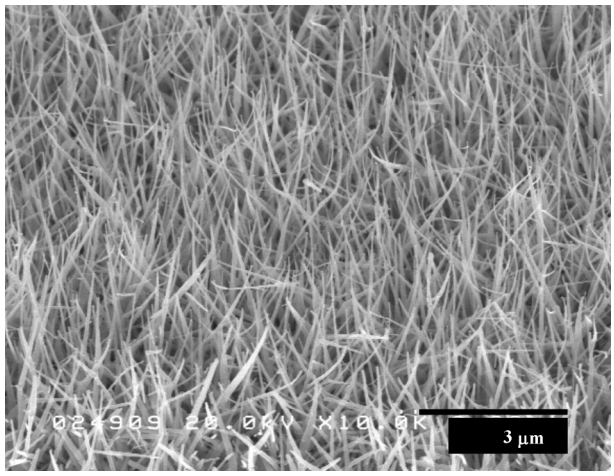

Fig. 3. A typical SEM image of ZnO nano-needles grown at 500 °C for 60 min under N_2 gas flow.

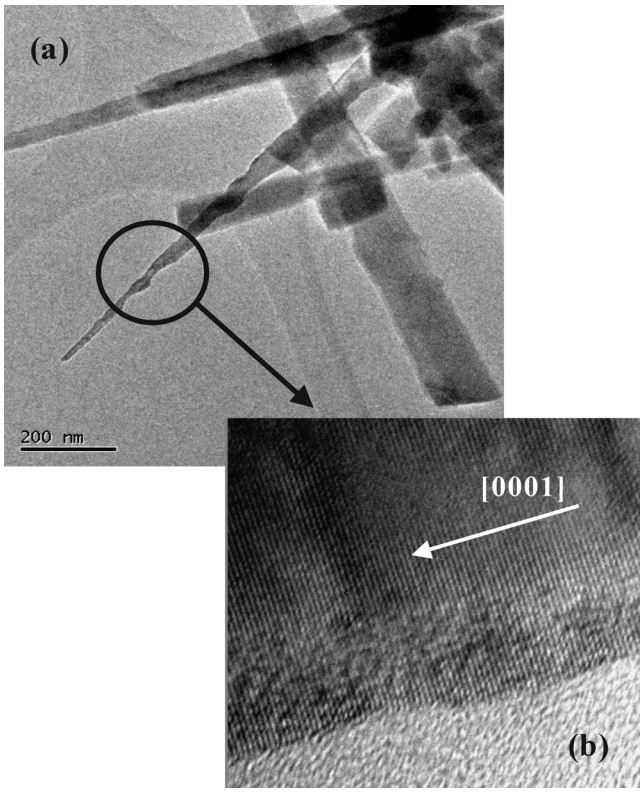

Fig. 4. TEM and HRTEM images of ZnO nano-needles grown at 500 °C for 60 min under N_2 gas flow.

picture clearly shows the growth of needle-shaped nanostructures, which have the largest and smallest diameters at the bottom and top of the structures, respectively. A high-resolution TEM image was also taken from a single ZnO nano-needle and is shown in Fig. 4(b). No crystalline defects, such as dislocations and stacking faults, are observed from the image. The spacing of adjacent lattice planes is 0.26 nm, corresponding to the distance between two (0 0 0 2) crystals planes [Yang et al., 2002; Li et al., 2002]. This means that the preferred growth direction of the ZnO nano-needles is <0 0 0 1>. Although not presented in this paper, the Raman measurement for the ZnO nano-needles also identified the growth of ZnO by observing the E_2 and E_1 (LO) modes of ZnO at 439 and 581 cm^{-1} [Wang et al., 2003]. Photoluminescence spectra showed the strong UV emission peak at 3.3 eV and a very weak green emission peak at 2.4 eV, also indicating the growth of good quality ZnO [Park et al., 2002].

It is interesting to note that our grown needle-shaped ZnO nanostructures are different from the shape of previously reported ZnO nanowires [Lee et al., 2003; Wang et al., 2002; Huang et al., 2001; Gao and Wang, 2002]. In the catalyst preparation process, the calcinations of $Ni(NO_3)_2$ at 500 °C under N_2 atmosphere might produce NiO nanoparticles on Si substrate surface since $Ni(NO_3)_2$ is completely decomposed at ~260 °C. In this experiment, no ZnO nanostructures were grown on the pure substrate without NiO. This means that NiO nanoparticles loaded on Si substrate surface play a key role for the growth of ZnO nano-needles, as observed in other nanowires and nanotubes growths.

The VLS growth mechanism has been universally employed to explain the growth of various nanowires and nanotubes over transition metal catalysts [Bonard et al., 2001; Lauhon et al, 2002]. In the mechanism, it was reported that nanosized catalyst provides a seed for the growth and the nanowires or nanotubes grow with a constant diameter throughout the reaction. In our experiments, however, the grown nanostructures showed a reduction of the diameter as the growth proceeded. Tseng et al. [Tseng et al., 2003] observed the growth of needle-like ZnO nanostructures over Ga-doped conductive ZnO film and explained that the reduction of the ZnO nanowire diameter is due to the decrease of the amount of reacting species (Zn or oxygen) supplied to reacting system during the reaction. In this growth system, Zn powders were placed in the reactor, but no oxygen was introduced into the reactor during the growth. Lyu et al. [2002] and Dai et al. [2002] reported the growth of ZnO nanowires without the supply of oxygen at similar growth condition. The literature suggested that the oxygen originates from moisture or oxygen remaining on the inside reactor wall. However, our experiment showed no growth of ZnO without NiO nanoparticles on Si surface. This means that oxygen in NiO can be an effective source to form ZnO. Although there are some reports on both transition metals and metal oxides such as Ni, Fe, NiO, FeO, etc., showing a good catalytic activity for the growth of semiconductor nanowires [Bonard et al., 2001; Lyu et al., 2003], it is assumed that NiO nanoparticles can directly participate in our growth of ZnO nano-needles. The size of NiO nanoparticles might be reduced due to the reaction with Zn by somehow. As the reaction proceeds, the amount of NiO nanoparticles decreases, whereas the length of ZnO nano-needles increases. In other words, NiO nanoparticles decrease in size as the reaction proceeds. Simultaneously, the diameter of ZnO nano-needles will reduce and consequently disappear from the grown nano-needles after the complete reaction. This is partly demonstrated with SEM and TEM observations, which showed no Ni or NiO formation on the tip of ZnO nano-needles. EDX analysis also identified the absence of Ni or NiO on the tip of the nano-needles.

To examine if the reaction of Zn and NiO is thermodynamically feasible, we did calculate the Gibbs free energy of the reaction at the growth temperature (500 °C).

$$Zn + NiO \rightleftarrows ZnO + Ni$$

The calculated free energy of the reaction was −24.0 kcal/mol at 500 °C, meaning that the reaction is to progress spontaneously at the temperature. The basic data used in the calculation were obtained from ref. [Knacke et al., 1991].

Summarizing the above experimental observations, the growth of the ZnO nano-needles may be interpreted by the following mechanism, fully depicted in Fig. 5. NiO nanoparticles are uniformly distributed across Si substrate surface after the calcinations. When Zn vapor passes over the Si surface, the NiO nanoparticles may provide seeds for the growth of ZnO nano-needles. The arrived Zn vapor absorbs into NiO nanoparticles to form a miscible liquid alloy of Zn-O-Ni at the growth temperature. The fluidization temperature of nano-sized melt particles is considerably lower than the melting point of bulk metal [Yan et al., 2000]. There, Zn will react with NiO to produce ZnO and Ni. Thus produced ZnO starts to precipitate on the bottom of the alloys to form ZnO nanostructures, whereas the reduced Ni moves to the surroundings of an NiO nanoparticle unreacted, because the melting point of Ni is lower than that of NiO [Lide, 1994]. The reaction proceeds until NiO nanoparticles are all consumed. The diameter of ZnO nano-needles might be the largest at the initial step of the growth, but it begins to decrease because of the reduction of NiO nanoparticle size by the reaction. Similarly,

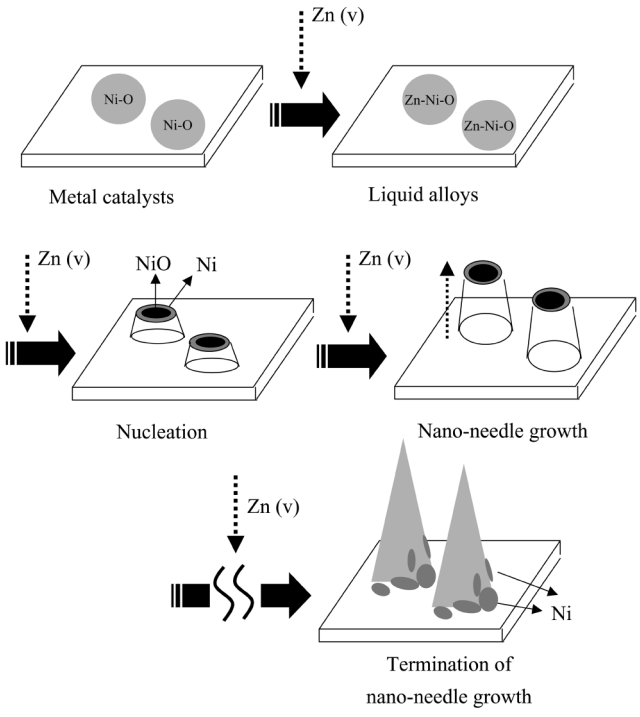

Fig. 5. The proposed growth mechanism of ZnO nano-needles.

the nano-needles diminish in diameter with the reaction and have sharpened tips. The growth of ZnO nano-needles stops when the NiO species are all exhausted by the reaction with Zn. EDX analyses at the upper and lower parts of a nano-needle reveal that the amount of Ni element on the surface of the nano-needle decreases with moving upward along the nano-needle from bottom (see Fig. 6). This result indirectly demonstrates that the amount of NiO decreases as the growth reaction proceeds since Ni is produced by the reduction of NiO. It is known that the growth rate of ZnO along (0 0 0 1) direction is much faster than the other growing directions [Pan et al., 2001]. The fast growth rate of ZnO nano-needles induces that liquid-phase Ni positioned on the surroundings of ZnO nanoparticles readily flows down the wall of the nano-needles.

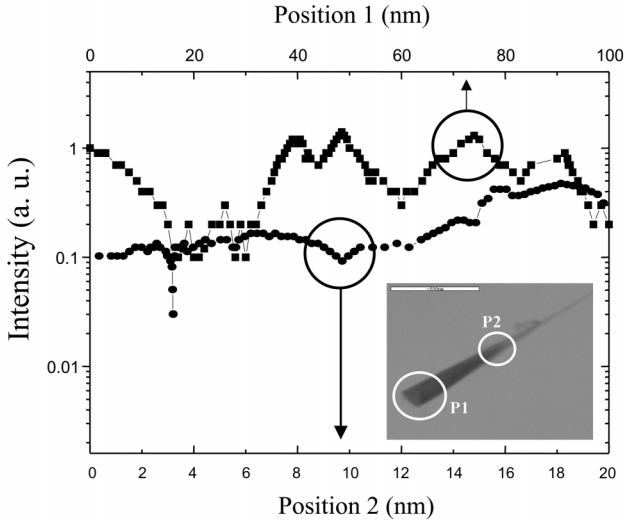

Fig. 6. The amount of Ni element on the surface of the nano-needle measured by EDX analysis (P1: bottom of the ZnO nano-needle; P2: top of the ZnO nano-needle).

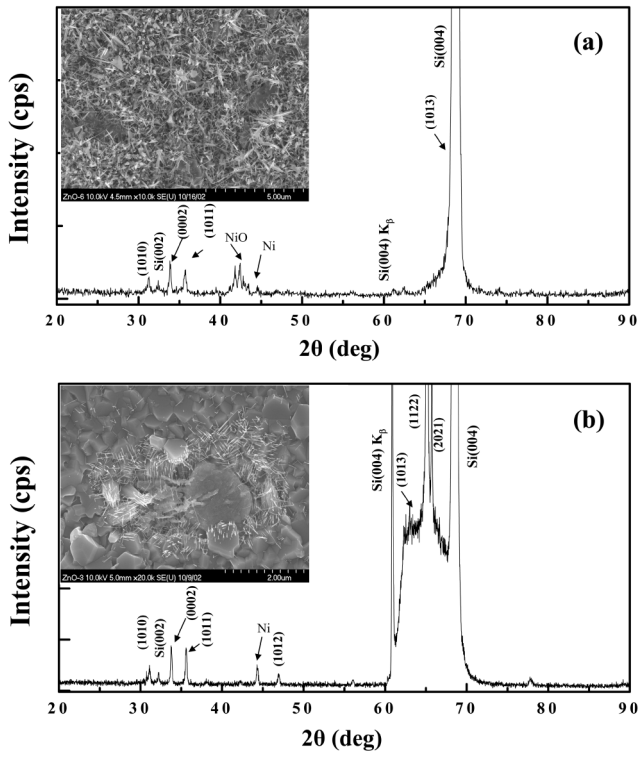

Fig. 7. Typical X-ray diffraction patterns of ZnO nano-needles grown at 500 °C under N_2 gas flow (a) for 30 min and (b) for 180 min, respectively, with their corresponding FE-SEM images.

Fig. 7(a) and (b) show the XRD spectra for the nanostructures grown at 30 and 180 min, respectively, with their FE-SEM images. From Fig. 2 and Fig. 7, it is seen that the morphology of the grown ZnO nanostructures changes with the growth time, from short ZnO nano-needles at 30 min to well-developed nano-needles at 60 min to micro-crystals at 180 min. The samples grown for 30 and 60 min exhibit both the NiO and Ni XRD peaks at 2θ=43.3 and 44.4, respectively, but Ni peak is only detected from the sample grown for 180 min. This demonstrates that our proposed mechanism reasonably explains the growth of the ZnO nano-needles. In order to understand the structural transformation of ZnO nano-needles to the micro-crystals, the ZnO nano-needles grown for 60 min were further annealed at 500 °C for 180 min only under N_2 atmosphere without Zn source. It is seen from Fig. 8 that the nano-needles disappear, whereas the micro-crystals appear. It seems that the ZnO nano-needles grow until 60 min growth time when both Zn source and NiO exist in the reactor, but the nano-needles thermally treated at the temperature without Zn source and NiO (after 60 min) begin to decompose or aggregate to be micro-crystals because of the termination of the growth reaction. This means that the growth of ZnO nano-needles is over at about 60 min in this growth condition and the extended growth time (180 min) at 500 °C results in the formation of ZnO micro-crystals by the aggregation or decomposition of the nano-needles due to the thermal effect.

Field emission characteristics were investigated for the ZnO nano-needles. The field emission characteristics were obtained in a vacuum chamber at 10^{-7} Torr. Gold-coated indium tin oxide (ITO) glass was used as an anode plate and the distance between ZnO sample and the anode glass was maintained to be 150 μm by using an alumina spacer. Fig. 9 shows the field emission current density from the ZnO nano-needles cathode as a function of the applied electric field.

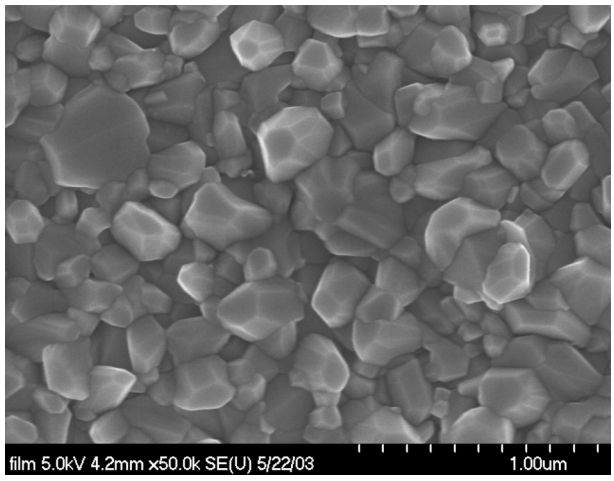

Fig. 8. A SEM image of ZnO nano-needles after annealing at 500 °C for 180 min under N_2 atmosphere.

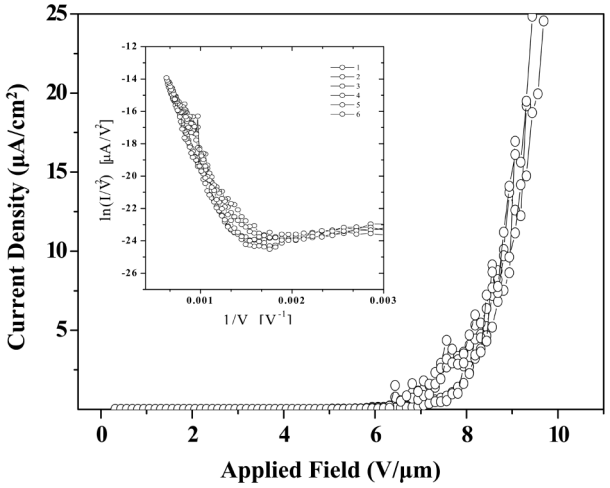

Fig. 9. Typical field emission characteristics of ZnO nano-needles with the F-N plot.

The initial turn-on field (the field to obtain 1 μA/cm^2) of ZnO nano-needles was observed to be about 8.87 V/μm. This is higher than typical carbon nanotubes' turn-on field (e.g. 1-2 V/μm for SWNT) [Zhu et al., 1999] and lower than other semiconductors such as gallium nitride (about 11 V/μm) [Chen et al., 2001]. The corresponding straight lines of the Fowler-Nordheim (F-N) plot shown in the inset of Fig. 9 indicate that the electron emission is proceeded by field emission. The field enhancement factor, β, was calculated from the slope of the F-N plot and the work function of ZnO (about 5.3 eV) [Minami et al., 1998]. The calculated β value was about 1090. This is much higher than that of ZnO nanowires [Lee et al., 2002], but is almost equal to that of ZnO nano-needles previously reported [Zhu et al., 2003]. The value of β is mainly dependent on the structural morphology of nanostructures and increases for nanostructures with a small diameter. Zhou et al. [2003] reported that the density of electric charge obtained from the sharp end of nano-structures is several times higher than that of the normal nanowire structures under the same experimental conditions. It is thought that our grown ZnO nano-needles will obviously generate high charge concentration when they are loaded by an electric field. This charge concentrating effect at the sharp end of the ZnO nano-needle may have the result of lowering electrical resistivity of the nano-material.

CONCLUSION

High-density hexagonal crystalline ZnO nano-needles were grown at 500 °C over NiO-coated Si substrate by a simple thermal evaporation of Zn powders in a homemade vertical CVD reactor. The diameter of the nano-needles decreased linearly from the bottom to the top. The bottom diameters of the nano-needles normally ranged from 20-100 nm and the lengths were in the range of 2-3 μm. It was considered that the vapor phase Zn passed over the Si surface reacted with NiO nanoparticles through a vapor-liquid-solid mechanism to form ZnO nano-needles. As the reaction proceeded, the diameter of ZnO nano-needles might have been reduced because of the reduction of NiO nanoparticle size. Our grown ZnO nano-needles showed that the turn-on field was found to be about 8.87 V/μm at a current density of 1 μA/cm^2 and the magnitude of field enhancement factor was about 1090.

ACKNOWLEDGMENT

This work was supported by the Brain Korea 21 Project in 2003.

REFERENCES

Ahn, S. H., Lee, S. H., Nahm, K. S., Suh, E. K. and Hong, M. H., "Catalytic Growth of High Quality GaN Micro-crystals," *J. of Crystal Growth*, **234**, 70 (2002).

Bonard, J. M., Weiss, N., Kind, H., Stockli, T., Forro, L., Kern, K. and Chatelain, A., "Tuning the Field Emission Properties of Patterned Carbon Nanotube Films," *Adv. Mater.*, **13**, 184 (2001).

Boo, J. H., Lee, S. B., Yu, K. S., Sung, M. M. and Kim, Y., "High Vacuum Chemical Vapor Deposition of Cubic SiC Thin Film on Si(001) Substrates Using Single Source Precursor," *Surface and Coating Technology*, **131**, 147 (2000).

Chen, C. C., Yeh, C. C., Chen, C. H., Yu, M. Y., Liu, H. L., Wu, J. J., Chen, K. H., Chen, L. C., Peng, J. Y. and Chen, Y. F., "Catalytic Growth and Characterization of Gallium Nitride Nanowires," *J. Am. Chem. Soc.*, **123**, 2791 (2001).

Choi, Y. C., Kim, W. S., Park, Y. S., Lee, S. M., Bae, D. J., Lee Y. H., Park, G. S., Choi, W. B., Lee, N. S. and Kim, J. M., "Catalytic Growth of -Ga_2O_3 Nanowires by Arc Discharge," *Adv. Mater.*, **12**, 746 (2000).

Dai, Y., Zhang, Y., Li, Q. K. and Nan, C. W., "Synthesis and Optical Properties of Tetrapod-like Zinc Oxide Nanorods," *Chem. Phys. Lett.*, **358**, 83 (2002).

Frederick, C. K. Au, Wong, K. W., Tang, Y. H., Zhang, Y. F., Bello, I. and Lee, S. T., "Electron Field Emission from Silicon Nanowires," *Appl. Phys. Lett.*, **75**, 1700 (1999).

Gao, P. and Wang, Z. L., "Self-Assembled Nanowire-Nanoribbon Junction Arrays of ZnO," *J. Phys. Chem.*, **106**, 12653 (2002).

Hu, J. Q., Li, Q., Wong, N. B., Lee, C. S. and Lee, S. T., "Synthesis of Uniform Hexagonal Prismatic ZnO Whiskers," *Chem. Mater.*, **14**, 1216 (2002).

Huang, M. H., Wu, Y. Y., Feick, H., Tran, N., Weber, E. and Yang, P., "Catalytic Growth of Zinc Oxide Nanowires by Vapor Transport," *Adv. Mater.*, **13**, 113 (2001).

Kim, K. C., Park, C. I., Roh, J. I., Nahm, K. S., Hahn, Y. B., Lee, Y. S. and Lim, K. Y., "Mechanistic Study and Characterization of 3C-SiC(100) Grown on Si(100)," *J. Electrochemical Society*, **148**(5), C383 (2001).

Kim, H. J. and Kim, W. S., "Estimation of Number of Surface Crystals on Sodium Fluoride Mother Crystal in Crystallization," *Korean J. Chem. Eng.*, **18**, 202 (2001).

Knacke, O., Kubaschewski, O. and Hesselmann, K., "Thermochemical Properties of Inorganic Substances I-II," Springer-Verlag Berlin: 2nd edition, 1455 (1991).

Lauhon, L. J., Gudiksen, M. S., Wang, D. and Lieber, C. M., "Epitaxial Coreshell and Coremultishell Nanowire Heterostructures," *Nature*, **420**, 57 (2002).

Lide, D. R., "CRC Handbook of Chemistry and Physics," 74th edition, CRC press, 4-36 (1993-1994).

Lee, C. J., Lee, T. J., Lyu, S. C., Zhang, Y., Ruh, H. and Lee, H. J., "Field Emission from Well-aligned Zinc Oxide Nanowires Grown at Low Temperature," *Appl. Phys. Lett.*, **81**, 3648 (2002).

Lee, J. S., Kang, M. I., Kim, S. S., Lee, M. S. and Lee, Y. K., "Growth of Zinc Oxide Nanowires by Thermal Evaporation on Vicinal Si(100) Substrate," *J. Crys. Growth*, **249**, 201 (2003).

Lee, S. H., Yu, S. G., Jeong, T. W., Heo, J. N., Kim, W. S., Lee, C. S., Lee, J. H., Kim, J. M., Kim, T. Y. and Nahm, K. S., "Field Emission of Zinc Oxide Nanostructure," 2003 MRS spring meeting Proceedings, **Volume 776**, Q11.35, San Francisco Marriott & Argent Hotels San Francisco, CA, April 21-25 (2003).

Li, Y., Meng, G. W., Zhang, L. D. and Philipp, F.," Ordered Semiconductor ZnO Nanowire Arrays and Their Photoluminescence Properties," *Appl. Phys. Lett.*, **76**, 2011 (2000).

Li, Y. B., Bando, Y., Sato, T. and Kurashima, K., "ZnO Nanobelts Grown on Si Substrate," *Appl. Phys. Lett.*, **81**, 144 (2002).

Liu, Z. W., Jun, K. W., Roh, H. S., Park, S. E. and Oh, Y. S., "Partial Oxidation of Methane over Nickel Catalysts Supported on Various Aluminas," *Korean J. Chem. Eng.*, **19**, 735 (2002).

Llewellyn, P. L., Chevrot, V., Ragai, J., Cerclier, O., Estienne, J. and Rouquerol, F., "Preparation of Reactive Nickel Oxide by the Controlled Thermolysis of Hexahydrated Nickel Nitrate," *Solid State Ionics*, **101-103**, 1293 (1997).

Lyu, S. C., Zhang, Y., Ruh, H., Lee, H. J., Shim, H. Y., Suh, E. K. and Lee, C. J., "Low Temperature Growth and Photoluminescence of Well-aligned Zinc Oxide Nanowires," *Chem. Phys. Lett.*, **363**, 134 (2002).

Lyu, S. C., Cha, O. H., Suh, E. K., Ruh, H., Lee, H. J. and Lee, C. J., "Catalytic Synthesis and Photoluminescence of Gallium Nitride Nanowires," *Chem. Phys. Lett.*, **367**, 136 (2003).

Minami, T., Miyata, T. and Yamamoto, T., "Work Function of Transparent Conducting Multicomponent Oxide Thin Films Prepared by Magnetron Sputtering," *Surface and Coatings Technology*, **108-109**, 583 (1998).

Nahm, K. S., Kim, T. Y. and Lee, S. H., "Catalytic Effect of Metal Elements on the Growth of GaN and Mg-doped GaN Micro-Crystals," *Korean J. Chem. Eng.*, **20**, 653 (2003).

Pan, Z. W., Dai, Z. R. and Wang, Z. L., "Nanobelts of Semiconducting Oxides," *Science*, **291**, 1947 (2001).

Park, W. I., Kim, D. H., Jung, S. W. and Yi, G. C., "Metalorganic Vapor-phase Epitaxial Growth of Vertically Well-aligned ZnO Nanorods," *Appl. Phys. Lett.*, **80**, 4232 (2002).

Park, W. I., Yi, G. C., Kim, M. Y. and Pennycook, S. J., "ZnO Nanoneedles Grown Vertically on Si Substrates by Non-Catalytic Vapor-Phase Epitaxy," *Adv. Mater.*, **14**, 1841 (2002).

Sohn, J. R. and Bae, J. H., "Characterization of Tungsten Oxide Supported on TiO_2 and Activity for Acid Catalysis," *Korean J. Chem. Eng.*, **17**, 86 (2000).

Sun, X. M., Chen, X., Deng, Z. X. and Li, Y. D., "A CTAB-Assisted Hydrothermal Orientation Growth of ZnO Nanorods," *Mater. Chem. Phys.*, **78**, 99 (2002).

Tseng, Y. K., Huang, C. J., Cheng, H. M., Lin, I. N., Liu, K. S. and Chen, I. C., "Characterization and Field-Emission Properties of Needle-like Zinc Oxide Nanowires Grown Vertically on Conductive Zinc Oxide Films," *Adv. Funct. Mater.*, **13**, 811 (2003).

Wang, Y. G., Lau, S. P., Zhang, X. H., Lee, H. W., Hng, H. H. and Tay, B. K., "Observation of Nitrogen-related Photoluminescence Bands from Nitrogen-doped ZnO Films," *J. Crys. Growth*, **252**, 265 (2003).

Wang, Y. W., Zhang, L. D., Wang, G. Z., Peng, X. S., Chu, Z. Q. and Liang, C. H., "Catalytic Growth of Semiconducting Zinc Oxide Nanowires and Their Photoluminescence Properties," *J. Crys. Growth*, **234**, 171 (2002).

Wu, Y., Fan, R. and Yang, P., "Block-by-Block Growth of Single-Crystalline Si/SiGe Superlattice Nanowires," *Nano Lett.*, **2**, 83 (2002).

Wu, Z. S., Deng, S. Z., Xu, N. S., Chen, J., Zhou, J. and Chen, J., "Needle-shaped Silicon Carbide Nanowires: Synthesis and Field Electron Emission Properties," *Appl. Phys. Lett.*, **80**, 3829 (2002).

Yan, H. F., Xing, Y. J., Hang, Q. L., Yu, D. P., Wang, Y. P., Xu, J., Xi, Z. H. and Feng, S. Q., "Growth of Amorphous Silicon Nanowires via a Solid-liquid-solid Mechanism," *Chem. Phys. Lett.*, **323**, 224 (2000).

Yang, P., Yan, H., Mao, S., Russo, R., Johnson, J., Saykally, R., Morris, N., Pham, J., He, R. and Choi, H. J., "Controlled Growth of ZnO Nanowires and Their Optical Properties," *Adv. Funct. Mater.*, **12**, 323 (2002).

Zheng, M. J., Zhang, L. D., Li, G. H. and Shen, W. Z., "Fabrication and Optical Properties of Large-scale Uniform Zinc Oxide Nanowire Arrays by One-step Electrochemical Deposition Technique," *Chem. Phys. Lett.*, **363**, 123 (2002).

Zhou, Z., Chu, L., Tang, W. and Gu, L., "Studies on the Antistatic Mechanism of Tetrapod-shaped Zinc Oxide Whisker," *J. Electrostat.*, **57**, 347 (2003).

Zhu, J. and Fan S., "Nanostructure of GaN and SiC Nanowires Based on Carbon Nanotubes," *J. Mater. Res.*, **14**, 1175 (1999).

Zhu, W., Bower, C., Zhou, O., Kochanski, G. and Jin, S., "Large Current Density from Carbon Nanotube Field Emitters," *Appl. Phys. Lett.*, **75**, 873 (1999).

Zhu, Y. W., Zhang, H. Z., Sun, X. C., Feng, S. Q., Xu, J., Zhao, Q., Xiang, B., Wang, R. M. and Yu, D. P., "Efficient Field Emission from ZnO Nanoneedle Arrays," *Appl. Phys. Lett.*, **83**, 144 (2003).